ORIGINAL ARTICLE

Transporters (OATs and OATPs) contribute to illustrate the mechanism of medicinal compatibility of ingredients with different properties in yuanhuzhitong prescription

Ze Wang[a,b], Haihua Shang[c,e], Yazhuo Li[b], Chen Zhang[b,f], Yan Dong[d], Tao Cui[a,b], Hongbing Zhang[b], Xiaoyan Ci[b], Xiulin Yi[b], Tiejun Zhang[b], Fengying Yan[b], Yaping Zhang[g], Xing Huang[h], Weidang Wu[b*], Changxiao Liu[a,b,c*]

[a]Tianjin University of Traditional Chinese Medicine, Tianjin 300193, China
[b]Biotechnology Center, Tianjin Institute of Pharmaceutical Research Co. Ltd., Tianjin 300193, China
[c]Tianjin Institute of Pharmaceutical Research New Drug Evaluation Research Co. Ltd., State Key Laboratory of Drug Release Technology and Pharmacokinetics, Tianjin 300031, China
[d]Chu Hsien-I Memorial Hospital, Tianjin Medical University, Tianjin 300134, China
[e]Shenyang Pharmaceutical University, Shenyang 110016, China
[f]Anhui Medical University, Hefei 230032, China
[g]Emergency Department, Zhongshan Hospital, Fudan University, Shanghai 200032, China
[h]Hefei Tianhui Hatching Technology Co. Ltd., Hefei 230032, China

Abstract   Various medicinal ingredients with different tastes are combined according to the theory of compatibility in Chinese materia medica to achieve a better efficacy, while the mechanism was not very clear. Here, the authors studied the interaction between ingredients and human transporters such as the kidney transporters OAT1 and OAT3, the liver transporters OATP1B1 and OATP1B3, and the intestine transporter OATP2B1 to discern the compatibility mechanism of ingredients with different tastes in the Yuanhuzhitong preparation (YHP) comprising *Corydalis yanhusuo* (CYH) and *Angelica dahurica*

*Corresponding authors.

   E-mail addresses: transporter2010@163.com (Weidang Wu), liuchangxiao_tjrp@163.com (Changxiao Liu).

OAT3;
OATP1B1;
OATP1B3;
OATP2B1

(AD), which could relieve pain by restraining the central system. The results show that tetrahydropalmatine (TDE), the major component of CYH, could be transported by OAT3 into kidney, OATP1B1 and OATP1B3 into liver, while imperatorin (IPT) and isoimperatorin (ISP), the two key components of AD, and AD extract showed strong inhibition to OAT1 and OAT3. What's more, AD extract also exerted strongly inhibition to human transporters OATP1B1 and OATP1B3. It was also detected that IPT, ISP, and AD extract significantly downregulated the expression of *Oatp1a1*, *Oatp1a4*, and *Oatp1b2* of liver in mice. The *in vivo* results show that the concentration of TDE in liver and kidney significantly decreased, while the TDE concentration in blood and brain were both significantly enhanced in the presence of IPT, ISP, and AD extract. These results suggest that the ingredients in AD with pungent taste could enhance the exposure of TDE in blood and brain by inhibiting the uptake of TDE in liver and kidney. That is to say, TDE with bitter taste could "flood up" into the central nervous system to play its therapeutic effect by the cut-off of that into liver and kidney in the presence of ingredients within AD. This paper not only proves the meridian distribution of CYH in liver and kidney with the role of OAT3, OATP1B1, and OATP1B3, but also illustrates how to improve the efficacy of CYH by reasonable compatibility with AD. This study may offer a valuable clue to illustrate the mechanism of compatibility theory.

1. Introduction

The theory of compatibility and property is one core content of Chinese materia medica theory. In order to reduce toxicity and enhance efficacy, Chinese herb or ingredients with different properties are combined according to the clinical needs. The ingredients with different properties play different roles in traditional Chinese medicine prescriptions (TCMPs). Yuanhuzhitong prescription (YZP), composed by *Corydalis yanhusuo* (CYH) and *Angelica dahurica* (AD), was proved effective in treatment of headache, collateral pain, and dysmenorrhea caused by stagnation of the circulation of vital energy and blood stasis[1]. The basic component for analgesic was monarch drug of CYH, while AD was the adjuvant to enhance the analgesic effect in YZP. CYH, was attributed to the liver and kidney meridians, has the effect of promoting blood circulation, invigorate vital energy and treat pain all over the body. However, the action site of CYH was central nervous system in brain, so it was a rational way to enhance the exposure of CYH in brain to get a better effect. AD, tasted pungent, has the function of spreading and ascending, which leads to the increase of brain exposure of CYH. Although AD has been proven to play an important role in reducing the toxicity and enhancing the efficacy of YZP, scientific explanation on the synergistic mechanism of AD is still needed. The active ingredients of traditional Chinese medicine (TCM) are the material basis for TCM to play therapeutic roles. Recently, it has been reported that there were about seven active components determined in YZP, which were also named quality markers (Q-markers)[2,3]. One of them was tetrahydropalmatine (TDE), belonging to alkaloids, which was proved one key central analgesic bioactive substance in CYH[3,4]. The other medicinal material, AD, tasted pungent, could expel fever and relieve pain[5]. The bioactivities ingredients in AD were mainly coumarin, methylcyclo-, tetradecane-substances, and so on, which were proved to express extensive pharmacological activities such as eliminating wind and dampness, detumescence, antipyretic action, spasmolysis, and relieving asthma[6]. Here, it was shown that the pharmacokinetics and pharmacodynamics of TDE would be substantially improved when combined with the AD extract. What's more, the area under the curve of drug−time (AUC) and the exposure of TDE in brain could be significantly increased when combined with AD. It was anticipated that the potential interaction mediated by transporters among different ingredients with different properties would be a future regulatory expectation during the process of absorption, distribution, metabolism, and excretion (ADME) *in vivo*. The important transporters such as OAT1, OAT3, OATP1B1, OATP1B3, MDR1, and BCRP may be involved in the ADME of compounds. As these transporters may be the important channels for compounds to selectively allow chemicals in and out of the cell or tissues, they play a crucial part in pharmacokinetics and pharmacodynamics of compounds. What's more, the pharmacokinetics and pharmacodynamics of one compound can be influenced by another one through transporters which was referred to as the drug−drug interaction (DDI) mediated by transporters. As all known, there were various ingredients with different tastes or properties in most TCMPs, it was not difficult to speculate that DDI could happen between different ingredients in TCMPs, which may provide a new protocol to illustrate the principle of combination among ingredients with different tastes or properties in TCMPs. Considering the complexity of DDI within YHP, the key components TDE in CYH and imperatorin (IPT), isoimperatorin (ISP) in AD were selected to insight the interaction mechanism.

In this paper, the authors found that TDE can be transported by OAT3, OATP1B1, and OATP1B3 into the intracellular from blood[7]. The compounds IPT, ISP, and the total extract of AD showed strong inhibition to OAT3, the important gateway for TDE and other compounds into kidney[8,9]. What's more, the total extract from AD exerted strong inhibition to OATP1B1 and OATP1B3 which were important transporters for hepatic uptake of TDE and other xenobiotic[10,11]. The results show that the accumulation of TDE in brain can be significantly increased when combined with AD by inhibiting its uptake and excretion by kidney and liver. Here, the authors tried to illustrate the reasonability of combination principle of CYH and AD in YZP through transporters mediating DDI, which may offer a new useful method to insight the mechanism of compatibility theory of ingredients with different tastes or properties in other TCMPs. The scientific explanation of the theory of compatibility and property will certainly further promote the reasonable, effective application of TCM.

2. Materials and method

2.1. Chemicals

The radix of *Angelicae dahuricae* was bought from Gansu Longshenrongfa Pharmaceutical Co., Ltd. (Lanzhou, China) and authenticated by Professor Tiejun Zhang (Department of Modern Chinese Materia Medica, Tianjin Institute of Pharmaceutical Research, Tianjin, China). Tetrahydropalmatine was obtained from Shanghai Jonln Reagent Co., Ltd. (Shanghai, China). Imperatorin and isoimperatorin were purchased from National Institute for the Control of Pharmaceutical and Biological Products (Beijing, China). The purities of all reference standards were over 98%. The materials for cell culture such as Dulbecco's modified phosphate buffer saline (DPBS), Dulbecco's modified Eagle's medium (DMEM), fetal bovine serum (FBS) and streptomycin with penicillin mixture (100-fold) were all purchased from Gibco Life Technologies (New York, NY, USA). The ^{3}H-estrone sulfate (^{3}H-ES) and ^{14}C-*para*-aminohippuric acid (^{14}C-PAH) were all obtained from American Radiolabeled Chemicals Incorporation (St. Louis, MO, USA). The Tri-Carb liquid scintillation counter with data analysis software were purchased from PerkinElmer, Inc (Change, USA). The transgene cell lines MDCK-Mock (blank plasmid carrier), MDCK-h*OAT1*, S2-WT, S2-h*OAT3*, HEK293-Mock, HEK293-h*OATP1B1*, HEK293-h*OATP1B3* were constructed and kindly offered by State Key Laboratory of Drug Delivery Technology and Pharmacokinetics (Tianjin, China).

2.2. Animals

Kunming mice (20−25 g, 6−8 week age) from Beijing Vital River Laboratory Animal Technology Co., Ltd. (Beijing, China, permit number SCXK 2016−0006) were allowed free access to water and food, but were in abrosia for 12 h (with water continuously) before the experiments. All the animal procedures were approved by Institutional Animal Care and Use Committee (IACUC) committee at Tianjin Institute of Pharmaceutical Research (TIPR) new drug assessment, according to Guide for the Care and Use of Laboratory Animals (National Research Council of the USA, 1996) and related ethical regulations of the China Academy of Chinese Medical Sciences (Beijing, China). The protocols were approved by the Animal Ethics Committee of Laboratory Animals at the Institute of Laboratory Animal Resources of Tianjin (Tianjin, China).

2.3. Cell culture

The culture medium for S2, MDCK and HEK293 cell lines as well as the cell lines overexpressing transporters was DMEM added with 10% FBS and 100 U/mL penicillin and 100 μg/mL streptomycin. The cell lines stored in liquid nitrogen were rapid thawed and revived in culture dishes with the diameter of 10 cm. After continuous passage for 2−3 generations in a humidified incubator at 33 or 37 °C and under 5% CO_2, the adherent cells were lysed by 0.25% trypsin, resuspended and seeded in 24-well culture plates at a density of $1.5 \times 10^5 - 2 \times 10^5$ cells/well. The cells proliferated to fully confluent in the wells may be used for inhibition and uptake studies[12].

2.4. Uptake experiments

In order to ensure models credible for use *in vitro*, the expression of the transporter genes in various transfected cells was determined by fluorescence quantitative real-time polymerase chain reaction (qRT-PCR). The sequences of the special primers for human transporters are shown in Table 1. The activities of transporter-overexpressing cells were also confirmed through the recognized substrate uptake assays. Briefly, the cells were incubated in the buffer solution containing 5 μmol/L ^{14}C-PAH for 2 min (hOAT1), 50 nmol/L ^{3}H-ES for 2 min (OAT3, OATP1B1, OATP1B3, and OATP2B1), taken the blank plasmid carriers such as MDCK-Mock, S2-Mock, HEK293-Mock as blank controls. And the transgene cell lines with great higher expression of transporter genes and higher transport activity (>2-fold activity of the blank control) would be selected as successful models *in vitro*.

To determine whether the ingredients (TDE, IPT, and ISP) were the substrates of transporters, cellular uptake of different ingredients in transporter-overexpressing cell lines and Mock cells lines were compared. Uptake experiments were performed as previously described[13,14]. The S2, MDCK, HEK293 cell lines overexpressing different transporters were seeded in culture plates with 24 wells at a density of 2×10^5 cells/mL. After the cells were cultured for 2 days, the cells were washed with one mL DPBS (containing 137 mmol/L NaCl, 3 mmol/L KCl, 8 mmol/L Na_2HPO_4, 1 mmol/L NaH_2PO_4, 1 mmol/L $CaCl_2$, and 0.5 mmol/L $MgCl_2$, pH 7.4) and then incubated in 1 mL DPBS in a water bath at 37 °C for 10 min. The former DPBS were then replaced by 0.5 mL fresh DPBS solution containing 100 μmol/L TDE, IPT, and ISP at 37 °C for 2−5 min. The uptake assay was terminated by taking away the reaction buffer solution and adding one mL icy DPBS to wash the cells for three times. The compounds of cells in each well were extracted with 0.4 mL methanol and then determined by HPLC−MS, and the protein concentration was determined by a BCA protein assay kit.

Substrate−transporter kinetics were also assayed. In the time-dependent study, the concentration of TDE was set as 10 μmol/L and the reactions were carried out for 0.5, 1, 2, 5, and 15 min respectively in different transporter models. In the concentration-dependent experiment, the concentrations of TDE were set as 0.03, 0.1, 0.3, 1, 3, and 10 μmol/L. Uptake kinetics of TDE were investigated by measuring the net accumulation (with subtracting the uptake of their relative Mock cells) of TDE at various concentrations within cells stably expressing transporters.

Table 1 The primers of human transporter gene used in the RT-PCR assays.

Primer	Sequence (5′−3′)
h*GAPDH*-Forward	GTCTCCTCTGACTTCAACAGCG
h*GAPDH*-Reverse	ACCACCCTGTTGCTGTAGCCAA
h*OAT1*-Forward	GGCTTCCTTGTCATCAACTCCC
h*OAT1*-Reverse	CACAGCAAGAGAGGTTCGGACA
h*OAT3*-Forward	CAACAGCACCAAGGACTCCATTG
h*OAT3*-Reverse	CTGTCAGACAGGTCTCCAAGCA
h*OATP1B1*-Forward	CGTAGAGCAACAGTATGGTCAGC
h*OATP1B1*-Reverse	TTGGCAATTCCAACGGTGTTCAG
h*OATP1B3*-Forward	GTCACCTTGTCTAGCAGGATGC
h*OATP1B3*-Reverse	GCATTCACCCAAGTGTGCTGAG
h*OATP2B1*-Forward	GTTTCGGCGAAAGGTCTTAGCAG
h*OATP2B1*-Reverse	CCATCCTGCTTCTTCGTGGACT

The transport parameters were calculated as Eq. (1):

$$V[(\text{pmol}/\min)/\text{mg protein}] = C \times v/t/P \tag{1}$$

where C represents the accumulated concentration of the uptake compound, v represents the volume of methanol used to extract the compound from the cells, t is the reaction time, and P is the protein concentration. The Michaelis−Menten constants $V_{\max}$ and K_m were calculated by fitting the data to the Michaelis−Menten equation Eq. (2):

$$V = V_{\max}/(1 + (K_m/[S])) \tag{2}$$

where $V_{\max}$ is the maximum transport rate, V is the transport rate, K_m is the substrate concentration resulting in half-maximal uptake rate, $[S]$ is the concentration of substrate.

2.5. Inhibition study

To evaluate the inhibition of TDE, IPT, ISP, and the total extract of AD on the activities of hOAT1, hOAT3, hOATP1B1, hOATP1B3, and hOATP2B1, TDE, IPT, ISP, and AD extract were dissolved in dimethyl sulfoxide (DMSO) at a concentration of 20 mmol/L or 10 mg/mL and diluted with PBS. The final concentration of dimethyl sulfoxide in the incubation PBS was adjusted to less than 0.5%. The cells were incubated in a solution containing 5 μmol/L ^{14}C-PAH for 5 min (hOAT1), 50 nmol/L ^{3}H-ES for 2 min (OAT3, OATP1B1, OATP1B3, and OATP2B1), in the absence or presence of various concentrations of TDE, IPT, ISP, and AD extract at 37 °C[15]. After incubation, the cells were washed with cold DPBS for three times to stop the procedure. And then, the treated cells were lysed with 0.5 mL sodium hydroxide solution (0.1 mol/L) and the total cell lysis were collected and mixed with five mL scintillation solution (Perkin−Elmer, Waltham, MA, USA). After mixed absolutely, the total radioactivity (DPM) of all the mixtures was determined by Tri-Carb 2910 Liquid Scintillation Counter (Perkin−Elmer)[15,16].

2.6. In vitro uptake in mice liver slices and kidney slices

In order to conform the similar role of transporters in mice, uptake studies using mice tissue slices were carried out as described previously[17]. Briefly, Kunming mice were anesthetized with urethane and their kidneys and livers were incised, decapsulated, and placed in ice-cold oxygenated incubation buffer (120 mmol/L NaCl, 16.2 mmol/L KCl, mmol/L CaCl$_2$, 1.2 mmol/L MgSO$_4$, and 10 mmol/L Na$_2$HPO$_4$, pH 7.5). About 30 mg of tissue slices were selected randomly and preincubated in a 24-well plate with 0.5 mL of incubation buffer in each well under a carbogen atmosphere at four or 37 °C for 5 min. After preincubation, the former incubation buffer was replaced with an incubation buffer containing tested compounds. Each slice was then removed rapidly from the incubation buffer, washed with ice-cold saline, drained on a filter paper, weighed, homogenized, and extracted with methanol using a single-step protein precipitation procedure. Uptake studies of TDE were carried out at a concentration of 10 μmol/L at four or 37 °C for 5, 10, and 30 min in the temperature- and time-dependent experiments. Probenecid (the confirmed inhibitor of OAT1 and OAT3) and rifampicin (the confirmed inhibitor of OATPs) were used to investigate the involvement of transporters in the tissue uptake of TDE. All the slices administrated with different agents were added 50% methanol by a rate of 200 mg tissue/mL and homogenized; 0.1 mL tissue homogenates and 0.1 mL diphenhydramine (100 μg/mL,

dissolved in methanol) would be taken out in a centrifuge tube and extracted by add 0.3 mL methanol; thereafter, the mixture was oscillated for 1 min, centrifuged at $16,000 \times g$ at 4 °C for 5 min and five μL supernatant was taken out for analysis by HPLC−MS.

2.7. The distribution of TDE in tissues of mice

The healthy mice were divided in to four groups, and they were orally administrated with 20 mg/kg TDE in the presence or absence of 20 mg/kg IPT, 20 mg/kg ISP, or 200 mg/kg AD extract respectively. The administrated mice were sacrificed by capillary blood collection method from the plexus veineux under the eyeball of mice which were narcotized by isoflurane at 1, 2, and 4 h after drug administration ($n = 6$). The blood, kidney, liver, and brain were also sampled at each time point. The TDE of each individual sample was extracted, and the concentrations were then determined through HPLC method.

2.8. Quantification of TDE in transfected cells and tissue slices using HPLC−MS

In this study, validated HPLC−MS-based methods were selected to quantify TDE in transfected cells, liver and kidney slices, and a triple-quadrupole mass spectrometer (AB SCIEX, Framingham, MA, USA) was interfaced via an electrospray ionization (ESI) probe with a 1200 liquid chromatograph (Agilent Technologies, Santa Clara, CA, USA). Chromatographic separation was achieved on a ZORBAX Eclipse XDB-C18 reversed-phase column (150 mm × 4.6 mm, 5 μm particle size; Dikma, Beijing, China) under a binary gradient of solvent A (0.1% formic acid) and solvent B (acetonitrile) at a flow rate of 0.5 mL/min and a temperature of 40 °C. The gradient of the mobile phase was as follows: linear decreased from 95% to 20% B at 0−4 min; maintained from four to 6.5 min and 95% B at 6.6−8.5 min. The mass spectrometer was operated in positive ESI mode, and quantification was performed using multiple-reaction monitoring of the transitions from m/z 356.50 to 192.20 for TDE and m/z 256.20 to 167.10 for diphenhydramine as the internal standard (IS). The linear range for measuring TDE in cells was from one to 300 nmol/L; the linear range for measuring TDE in mice tissues was from 100 to 10,000 μg/L; accuracy, precision, recovery, and stability tests all met the requirements of biological samples (Supporting Information). The conditions for mass spectrometric analysis were as follows: nebulizing gas flow, three L/min; heating gas flow, 10 L/min; interface temperature, 300 °C; DL temperature, 50 °C; heat block temperature, 400 °C; drying gas flow, 10 L/min. Samples with concentrations above the higher limit of quantification were diluted with a blank tissue homogenate and then reanalyzed.

2.9. Quantification of TDE in tissues of mice using HPLC analysis

2.9.1. Extraction of drugs from mice tissues
The drug extraction procedure was modified from those previously described[6]. Liver, spleen, kidney, and brain were weighted for wet weight and then cut into small pieces. The tissue homogenates were prepared by adding pre-cooled normal saline to tissue at a ratio of 5:1 (v/w) and then separately by a homogenizer (Sonifier 450; Branson Ultrasonics, Branson, MS, USA). Then the obtained homogenates were stored at −80 °C until analysis.

An internal standard method was adopted to determine the concentration of TDE in the tissue samples. An aliquot of 200 μL of tissue homogenate was mixed with 50 μL of internal standard solution (corydaline; CDE, 5 mg/L) in a glass tube and vortex-mixed for 30 s. Then one mL *n*-hexane-2/propanol (95/5) was added in the glass tube, and then vortex-mixed for 3 min; the obtained mixture was centrifuged at $16,000 \times g$ for 15 min. The upper organic layer was transferred to a clean glass centrifuge tube and dried under a stream of nitrogen at 40 °C. The dried samples were reconstituted with 100 μL mobile phase, shocked in vortex for 1 min, and then centrifuged for 5 min at $16,000 \times g$ at 4 °C. After centrifugation, 100 μL supernatant was kept at -80 °C before HPLC analysis.

2.9.2. Quantification of TDE in mice tissues using HPLC

The samples were analyzed by Agilent 1100 HPLC system (Agilent Technologies, Lexington, KY, USA). The Diamosil C18 column (200 mm × 4.6 mm, 4.5 μm; Dikma, Beijing, China) was used. The working conditions were as follows: the mobile phrase was acetonitrile/0.34% KH_2PO_4 (25:75); column temperature was 30 °C; the flow rate was one mL/min; the injection sample volume was 40 μL; the detective wave length was 280 nm.

2.10. RT-PCR analysis

Animals were orally administrated with TDE at a dosage of 20 mg/kg in the presence or absence of 20 mg/kg IPT, ISP, or 200 mg/kg AD extract were sacrificed by taking off the cervical spine. The kidney and liver of the mice were collected and pulverized in liquid nitrogen. And the total RNA was extracted by TRIzol® reagent (Tiangen, Beijing, China). The expression levels of m*Oat1*, m*Oat3*, m*Oatp1a1*, m*Oatp1a4*, and m*Oatp1b2* were analyzed by qRT-PCR and the procedure was according to the protocol of the manufactures. The sequences of the special primers for mice are shown in Table 2. The cDNA was amplified by using SYBR® Premix Ex Taq™ kit (Roche, Basel, Switzerland) and Eppendoff (Applied Biosystems, Foster City, CA, USA). The requirements for PCR were as follows. The temperature for prime denaturation was 95 °C for 30 s, and 40 cycles contained three steps: denaturation at 95 °C for 5 s, annealing at 55 °C for 15 s, and extension at 60 °C for 20 s. Gene expression levels were calculated by the comparative C_t method as described previously and the values were normalized to endogenous reference m*Gapdh*. The formula was as Eq. (3):

Table 2   The primers of mice transporter gene used in the RT-PCR assays.

Primer	Sequence (5′−3′)
m*Gapdh*-Forward	CATCACTGCCACCCAGAAGACTG
m*Gapdh* -Reverse	ATGCCAGTGAGCTTCCCGTTCAG
m*Oat1*-Forward	GAAAGGCTGTCTGGCTTCCTCT
m*Oat1*-Reverse	ATCAGTGGGCTCACTATGCTGC
m*Oat3*-Forward	AGGCTCTGAAGACACTCCAACG
m*Oat3*-Reverse	ACCTTGGCTGAGGTGATGTCCT
m*Oatp1a1*-Forward	GCTGTTCAGTCTTACGAGTGTGC
m*Oatp1a1*-Reverse	CAAGGCATACTGGAGGCAAGCT
m*Oatp1a4*-Forward	GCCAAAGAGGAGAAGCACAGAG
m*Oatp1a4*-Reverse	AAAGGCATTGACCTGGATCACAC
m*Oatp1b2*-Forward	GCAATGATCGGACCAATCCTTGG
m*Oatp1b2*-Reverse	CCAACGAGCATCCTGAGGAGTT

Table 3   The mRNA levels and transport activities of h*OAT1*, h*OAT3*, h*OATP1B1*, h*OATP1B3*, and h*OATP2B1* in the transfected cells.

Relative mRNA expression		Uptake rate (pmol/mg protein/min)	
		Control	Control + inhibitor
MDCK-MOCK	ND	1.66 ± 0.84	2.01 ± 0.37
MDCK-h*OAT1*	0.0903	$19.2 \pm 1.38^{**}$	6.5 ± 0.74
S2-MOCK	ND	0.11 ± 0.011	0.10 ± 0.019
S2-h*OAT3*	0.0089	$0.62 \pm 0.015^{**}$	0.29 ± 0.17
HEK293-MOCK	ND	0.11 ± 0.013	0.11 ± 0.012
HEK293-h*OATP1B1*	0.0074	$1.13 \pm 0.11^{**}$	0.35 ± 0.14
HEK293-h*OATP1B3*	0.1431	$0.52 \pm 0.017^{**}$	0.24 ± 0.13
HEK293-h*OATP2B1*	0.0160	$0.46 \pm 0.011^{**}$	0.19 ± 0.034

Mock, the wild type cell line. MDCK-h*OAT1*, the MDCK cell line overexpressing human OAT1; S2-h*OAT3*, the S2 cell line overexpressing human *OAT3*; HEK293-h*OATP1B1*, the HEK293 cell line overexpressing human *OATP1B1*; HEK293-h*OATP1B3*, the HEK293 cell line overexpressing human *OATP1B3*; HEK293-h*OATP2B1*, the HEK293 cell line overexpressing human *OATP2B1*. The uptake of model substrate in transporter cells and Mock cells. The cells were incubated in a solution containing 5 μmol/L ^{14}C-PAH for 2 min (hOAT1), 50 nmol/L ^{3}H-ES for 2 min (hOAT3, hOATP1B1, hOATP1B3 and hOATP2B1). ND, not detected. The values are mean ± SD ($n = 3$); $^{**}P < 0.01$. Statistical analysis was performed using Student's paired *t*-tests.

$$Et = 2^{-[(Ct_{21}-Ct_{20})-(Ct_{11}-Ct_{10})]} \tag{3}$$

In the formula, the gene expression level in the control sample (the group administrated by TDE alone) were defaulted to 1. Et was the relative expression level of the target genes; C_{t11} indicated the cycles of tested gene in the control group when its amplification curve accessed to the threshold value of fluorescence signal, C_{t10} indicated the cycles of m*Gapdh* in the control group when its amplification curve accessed to the threshold value of fluorescence signal; C_{t21} indicated the cycles of tested gene in other groups when its amplification curve accessed to the threshold value of fluorescence signal, C_{t20} indicated the cycles of m*Gapdh* in the corresponding group when its amplification curve accessed to the threshold value of fluorescence signal.

2.11. Statistical analysis

The independent samples *t*-test was used for comparisons by SPSS 15.0 software (SPSS, Chicago, IL, USA). Values of $P < 0.05$ were considered statistically significant.

3. Result

3.1. The cellular uptake

The expression of the transporter gene in various transfected cells was determined by qRT-PCR. The results show that the expressions of h*OAT1*, h*OAT3*, h*OATP1B1*, h*OATP1B3*, and h*OATP2B1* in transfected cells were significantly higher than that in Mock cells (normalized to h*GAPDH*). The transport activities of the transporter cells were confirmed by comparing the uptake of model substrates in transporter cells with that of Mock cells. Data showed that the uptake of ^{14}C-PAH in MDCK-h*OAT1* cells was

11.5-fold higher than that in Mock cells. The accumulation of ^{3}H-ES in S2-h*OAT3*, HEK293-h*OATP1B1*, HEK293-h*OATP1B3*, and HEK293-h*OATP2B1* cells was 5.6-fold, 10.3-fold, 4.7-fold, and 4.2-fold higher than that in Mock cells respectively (as shown in Table 3).

In order to determine whether TDE, IPT, and ISP can be transported by different transporters, 100 µmol/L TDE, IPT, and ISP were administrated to MDCK-h*OAT1*, S2-h*OAT3*, HEK293-h*OATP1B1*, HEK293-h*OATP1B3*, and HEK293-h*OATP2B1* cell lines, as well as the wild type cell lines (MDCK-Mock, S2-Mock, and HEK293-Mock). The results show that the accumulations of TDE, IPT, and ISP in MDCK-h*OAT1* were about 1.25-, 4.92-, and 3.40-fold higher than that in the MDCK-Mock cell line (as shown in Fig. 1A), suggesting that IPT and ISP were the substrates of hOAT1 but TDE not (>2-fold of that for wild type). As for hOAT3, the accumulation of TDE, IPT, and ISP in S2-h*OAT3* was about 2.25-, 4.92-, and 3.40-fold higher than that of the wild type (S2-Mock, as shown in Fig. 1B), from which we can infer that TDE, IPT, and ISP could be transported by hOAT3. TDE, IPT, and ISP could largely accumulate in the h*OATP1B1*-overexpressed cell lines compared to the wild type cell lines (as shown in Fig. 1C), suggesting that TDE, IPT, and ISP could be transported by hOATP1B1. The results also show that the accumulation of TDE (3.31-fold) in HEK293-h*OATP1B3* cell lines was more than 2-fold than that in HEK293 wild type cell lines but there were no significant differences in the two kinds of cell lines treated with IPT and ISP (as shown in Fig. 1D), suggesting that TDE was the substrate of OATTP1B3 but IPT and ISP not. As the accumulations of TDE, IPT, and ISP in HEK293-hOATP2B1 cell line were all less than 2-fold than that in HEK293 wild type cell line as shown in Fig. 1E, so they were not substrates of transporter hOATP2B1. These results implicated that hOAT3 played an important role for TDE, IPT, and ISP to enter kidney; besides, the two transporters hOATP1B1 and hOATP1B3 both attributed to the uptake of TDE by human liver. Nevertheless, the transporter OATP2B1 seemed to show no attribution for the transport of TDE, IPT, and ISP. What's more, the results also suggest the potential possibility of drug−drug

interaction between TDE and IPT, ISP as well as the other ingredients in AD extract.

In order to further prove transporters involved in the transport of TDE, the substrate−transporter kinetics studies between TDE and hOAT3 (Fig. 2A and B), hOATP1B1 (Fig. 2C and D), and hOATPB3 (Fig. 2E and F) were carried out. The results of substrate−transporter kinetics show that the uptakes of TDE in cells overexpressing h*OAT3*, h*OATP1B1*, and h*OATP1B3* were much higher than that in Mock cells in time- and concentration-dependent manners. Eadie−Hofstee plot analysis indicated that the K_m and V_{max} values of TDE were 1.44 µmol/L, 188.45 pmol/mg protein/min for hOAT3, 18.59 µmol/L, 208.68 pmol/mg protein/min for hOATP1B1, 6.72 µmol/L, 512.09 pmol/mg protein/min for hOATP1B3, respectively.

### 3.2. The inhibition to transporters

In order to evaluate the inhibition of TDE, IPT, ISP and the total extracts AD to the transporters, 100 µmol/L TDE, IPT, and ISP were administrated to MDCK-h*OAT1*, S2-h*OAT3*, HEK293-h*OATP1B1*, HEK293-h*OATP1B3*, and HEK293-h*OATP2B1* cell lines in the presence of the recognized substrate such as ^{14}C-PAH and ^{3}H-ES. The results show that IPT, ISP, and AD significantly inhibited the activity of hOAT1 and hOAT3 in strength (as shown in Fig. 3A and B). Although the 100 µg/mL AD extract exerted strong inhibition to hOATP1B1 and hOATP1B3, IPT and ISP showed weak or no inhibition to hOATP1B1 (Fig. 3C), hOATP1B3 (Fig. 3D), and hOATP2B1 (Fig. 3F). It was suggested that there may be other unknown components in AD extracts which could strongly inhibit the activity of hOATP1B1 and hOATP1B3.

In order to further verify the inhibitory ability of different components in AD to different transporters, the IC_{50} of IPT, ISP, or AD extract to the uptake of model substrate in different cell lines were also determined. The results show that IPT, ISP, and AD extract exerted strong inhibition on the uptake of ^{14}C-PAH in MDCK-h*OAT1* cell line, the IC_{50} values were 31.71 µmol/L, 26.78 µmol/L, and 1.18 mg/L as shown in Fig. 4A−C. What's
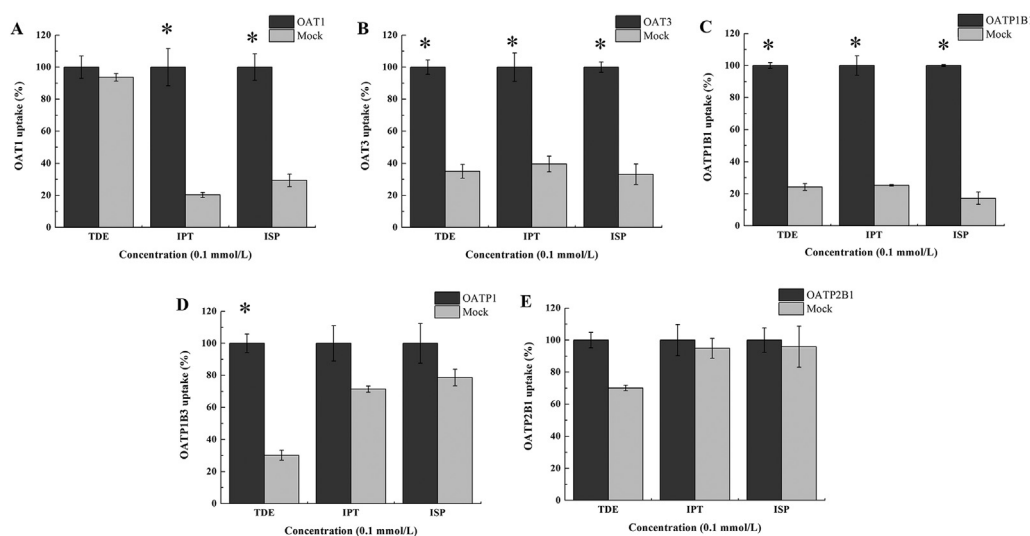
Figure 1 The uptake of different ingredients by human transporters hOAT1 (A), hOAT3 (B), hOATP1B1 (C), hOATP1B3 (D), and hOATP2B1 (E). The values are mean ± SD ($n = 3$); $^*P < 0.05$. Statistical analysis was performed using the independent samples *t*-test by SPSS 15.0 software (SPSS, USA).
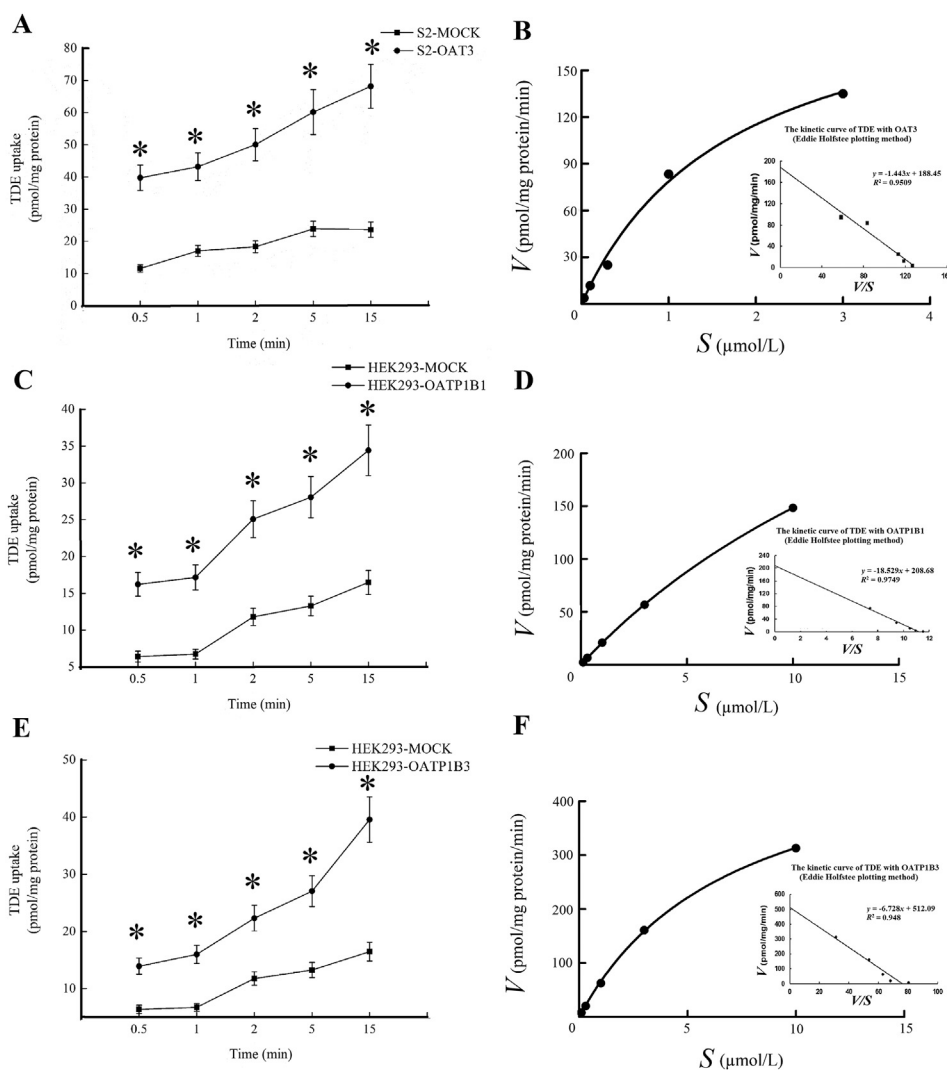
Figure 2 Time- and concentration-dependent uptake of TDE in S2-h*OAT3* (A) and (B), HEK293-h*OATP1B1* (C) and (D), HEK293-h*OATP1B3* (E) and (F), and Mock cells. In the time profiles, the uptake of TDE was examined at a concentration of 1 μmol/L. The concentration-dependent uptake was measured at TDE concentrations between 0.03 and 10 μmol/L for 2 min at 37 °C. The values are mean ± SD ($n = 3$); $^*P < 0.05$. Statistical analysis was performed using the independent samples *t*-test by SPSS 15.0 software (SPSS, USA).

more, IPT ($IC_{50} = 2.74$ μmol/L), ISP ($IC_{50} = 11.7$ μmol/L), and AD ($IC_{50} = 3.17$ μg/mL) expressed significant inhibition to the uptake of ^{3}H-ES in S2-h*OAT3* cell line. Although IPT and ISP expressed no or very weak inhibition to hOATP1B1 or hOATP1B3, AD extract could strongly inhibit the uptake of ^{3}H-ES in the HEK293-h*OATP1B1* and HEK293-h*OATP1B3* cell lines in a dose-dependent manner as shown in Fig. 4E and F. From Fig. 4E and F, 10.38 and 6.38 μg/mL AD could inhibit the activity of hOATP1B1 and hOATP1B3 to half of the maximum respectively.

As TDE could enter kidney and liver in the assistance of hOAT3, hOATP1B3, and hOATP1B3, while IPT, as well as AD extract, exerted significant inhibition to hOAT3 and the AD extract also showed strong inhibition to hOATP1B1 and hOATP1B3. It was suggested that the distribution of TDE in kidney and liver may decrease when combined with IPT, ISP, and AD extract. As a result, the decrease flux of TDE in kidney and liver may contribute a higher flux and longer circulation of TDE in blood, which was beneficial for more TDE to be transported through the blood−brain barrier for a better abirritation.

3.3. The uptake in kidney and liver slices of mice in vitro

In order to prove transporters of kidney and liver of mice, the fresh kidney and liver slices of mice were taken as uptake models *in vitro*. Results show that the uptake of TDE (10 μmol/L) at 37 °C was markedly increased in 30 min, compared with the uptake at 4 °C. In addition, a significant difference was observed. The accumulation of TDE at 37 °C was approximately 2.3-fold greater than that at 4 °C in the liver slices ($P < 0.01$, as shown in Fig. 5). Meanwhile, the effects of IPT, ISP, and AD extract on the uptake of TDE in kidney and liver slices were also evaluated. The results show that IPT, ISP, and AD extract exerted significant inhibition on the uptake of TDE in liver slices and kidney slices, as shown in Fig. 5A and B, respectively. Moreover, the effects of inhibitors on the TDE uptake were investigated in mice tissue slices. Rifampicin (an OATP inhibitor), could inhibit the primary hepatic uptake of TDE in mice liver slices, and probenecid (an OATs inhibitor) could inhibit the primary renal uptake of TDE in mice kidney slices. These results suggest that IPT, ISP, and AD extract
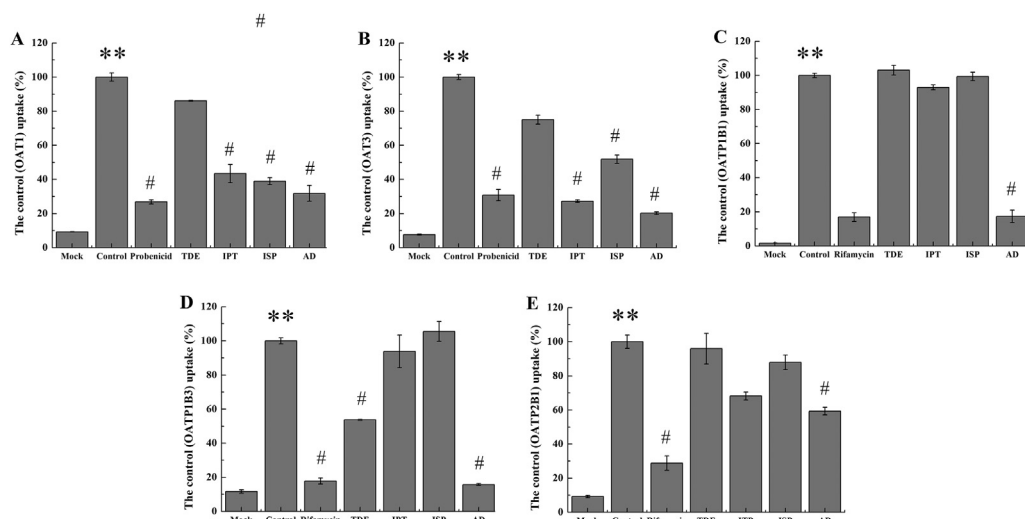
Figure 3 The inhibition of different ingredients TDE, IPT, ISP and AD extract to human transporters OAT1 (A), OAT3 (B), OATP1B1 (C), OATP1B3 (D), and OATP2B1 (E). The dosage of TDE, IPT and ISP was 100 μmol/L and the dosage of AD extract was 100 mg/L *in vitro*. The values are mean ± SD ($n = 3$); $^*P < 0.05$. $^{**}P < 0.01$ *vs.* mock; $^{\#}P < 0.05$, $^{\#\#}P < 0.01$ *vs.* control. Statistical analysis was performed using one-way ANOVA with Bonferroni's *post-hoc* test.

may decrease the uptake of TDE in kidney and liver slices by inhibiting the activities of OATs or OATPs of mice.

3.4. Tissue distribution of TDE

As IPT, ISP, and AD extract showed inordinately inhibition to the activity of hOAT3, hOATP1B1, and hOATP1B3, suggesting that they may change the distribution of TDE *in vivo*, the distribution of TDE in brain, liver, kidney and serum was determined at 1, 2, and 4 h after administration with TDE in the presence or absence of IPT, ISP, or AD extract in Kunming mice. The results show that the concentration of TDE in blood and brain of mice administrated with TDE in the presence of IPT, ISP, or AD extract for 1, 2, and 4 h was significantly enhanced compared to that in mice
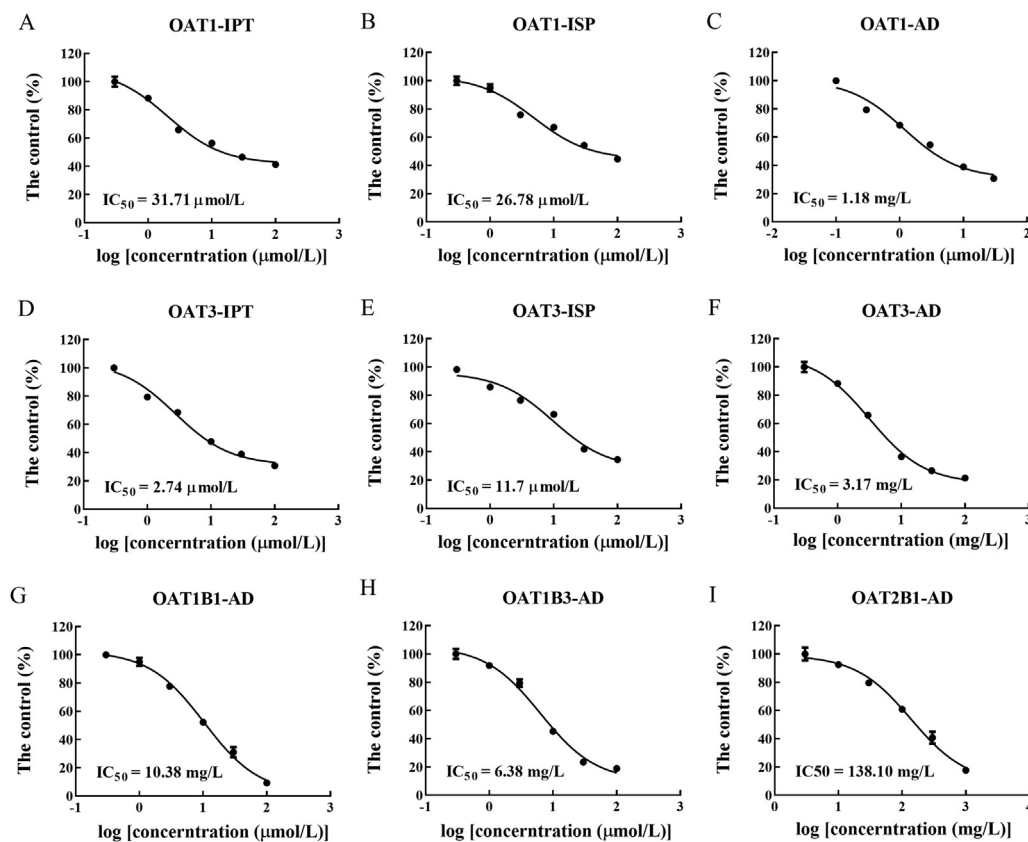
Figure 4 The inhibition of IPT, ISP or AD extract to the uptake of TDE in different cell lines which overexpressed h*OAT1* (A)−(C), h*OAT3* (D)−(F), h*OATP1B1* (G), h*OATP1B3* (H), h*OATP2B1* (I). The values are mean ± SD ($n = 3$).
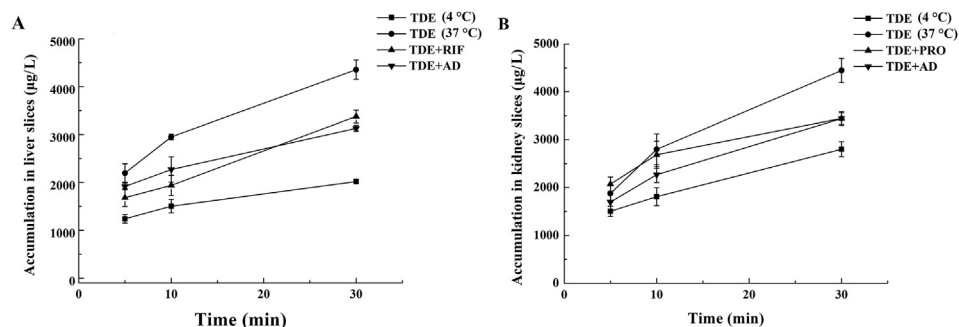
Figure 5 The accumulation of TDE in the presence or absence of IPT, ISP, or AD extract in mice liver slices (A), and kidney slices (B). The values are mean ± SD ($n = 3$); $^{*}P < 0.05$. Statistical analysis was performed using one-way ANOVA with Bonferroni's *post-hoc* test.

administrated with TDE alone, while the accumulation in kidney and liver was significantly decreased ($P < 0.05$) as shown in Fig. 6. The results suggest that IPT, ISP, or AD extract may decrease the distribution of TDE in kidney and liver which resulted in the enhancement of the exposure of TDE in blood and brain. It may be interpreted as that when the total TDE pool in mice was no longer increase after administration, more influx may accumulation into other branch pools like blood and brain if the influx of TDE into the branch pools such as kidney and liver decreased.

3.5. The RNA levels of different transporters in kidney and liver of mice

Although the expressions of hOATP1B1, hOATP1B3, and hOATP2B1 were not detected in the liver of mice due to species differences, the tissue specificity and substrate recognition of mOATP1A1, mOATP1A4, and mOATP1B2 are very similar to human OATP1B1, OATP1B3, and OATP2B1[18]. To testify whether mouse was a suitable model for studying liver and kidney transporters, the authors quantified the mRNA expression of different transporter gene, including m*Oat1*, m*Oat3*, m*Oatp1a1*, m*Oatp1a4*, and m*Oatp1b2* by the real-time quantitative PCR (qRT-PCR) using SYBR Green with designed primers. Data show that the mRNA levels of m*Oat1* and m*Oat3* were very low, while the mRNA levels of m*Oatp1a1*, m*Oatp1a4*, and m*Oatp1b2* were expressed at high levels in mouse liver (as shown in Fig. 7A). Additionally, the mRNA levels of m*Oat1* and m*Oat3* were highly expressed, while the mRNA levels of m*Oatp1b1*, m*Oatp1a4*, and m*Oatp1b2* were very low in mice kidney (as shown in Fig. 7B). These results indicate that the transporters in the mouse kidney and liver exerted parallel roles in the disposition of TDE.

To investigate the interaction mechanism between IPT, ISP, and AD extract and TDE, the mRNA levels of m*Oat1*, m*Oat3*, m*Oatp1a1*, m*Oatp1a4*, and m*Oatp1b2* in the kidneys and livers of mice treated with TDE in the presence or absence of IPT, ISP, and AD extract were analyzed by qRT-PCR. As the results shown, there were no difference to be detected on the mRNA levels of m*Oat1* and m*Oat3* in all mice treated with TDE or others (Fig. 7C). The results infer that IPT, ISP, or AD exerted no inhibition to the expression of m*Oat1* or m*Oat3*. However, mRNA levels of m*Oatp1a1* were markedly decreased to 22%, 37%, and 24% in the liver of animals treated with TDE in the presence of IPT, ISP and AD extract separately, compared to mice treated with TDE (Fig. 7D); what's more, the mRNA levels of m*Oatp1a4* were markedly decreased to 36%, 61%, and 49% in the liver of animals

treated with TDE in the presence of IPT, ISP, and AD extract separately, compared to that of mice treated with TDE alone; meanwhile, compared to mice treated with TDE alone, the m*Oatp1b2* mRNA levels were also significantly decreased to 61%, 50%, and 35% in the liver of mice treated with TDE combined with IPT, ISP, and AD extract separately. From the results, it was not difficult to infer that IPT, ISP, and AD extract may decrease the distribution of TDE in liver through down regulating the expression of m*Oatp1a1*, m*Oatp1a4*, and m*Oatp1b2* of mice, while IPT, ISP, and AD extract may decrease the uptake of TDE in kidney mainly by competitively inhibit the activities of mOAT1 and mOAT3.

4. Discussion

Chinese medicine is an important part of Chinese traditional culture and has been making outstanding contributions to the reproduction and survival of the Chinese nation. It has developed many unique theories such as the compatibility theory, the five tastes theory, meridians theory, and the indication of syndromes, some of which are not yet elucidated by modern technology. The compatibility theory of Chinese medicine is the essence in the prescriptions of traditional Chinese medicine and fully demonstrated the selectivity of drug therapeutic effects. Additionally, the five tastes theory is the basic theory for medicinal materials with different properties to compose a prescription. Meridian distribution theory is a core principle, which means that Chinese traditional herbs with different properties may act on certain targeted organs or tissues with preference, thus raise the specificity of medicine and strengthen the therapeutic effects[19]. As there were no appropriate methods to illustrate the immanent scientificity of the five tastes theory, it was always believed some mystique.

In recent years, more and more modern technologies, including the methods of genomics, proteomics, and metabolomics, were explored to illustrate the theories and laws of Chinese medicine. There were many compounds to be detected in the traditional Chinese prescriptions through HPLC−MS, GC−MS, nuclear resonance spectroscopy (NMR), and so on, and these compounds were the chemical basis and nature of the Chinese medicine for the pharmacological actions[20]. Moreover, with the rapid development of sensitive detection technology and biotechnology, various new tools also provide choices to elucidate the mechanism of compatibility theory for TCM from different perspectives: (1) LC−MS, GC−MS, or NMR were used to monitor the changes in ingredients during processing *in vivo*[21]. (2) *In vitro* cell models were used to explain the changes in permeability caused by the
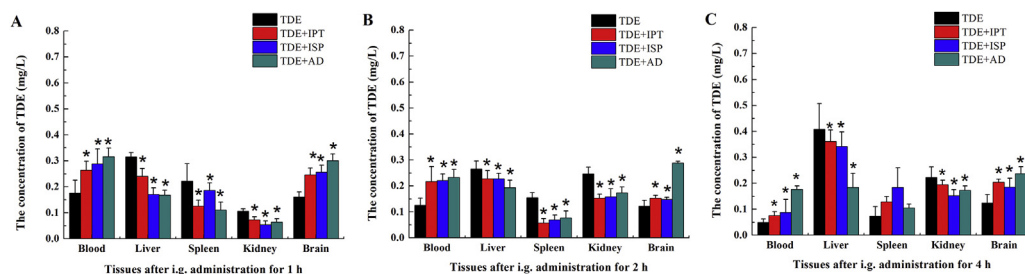
Figure 6 The tissue distribution of TDE in the presence or absence of IPT, ISP, or AD extract in mice after administrated for 1 h (A), 2 h (B), and 4 h (C). The values are mean ± SD ($n = 6$); $^*P < 0.05$. Statistical analysis was performed using one-way ANOVA with Bonferroni's *post-hoc* test.
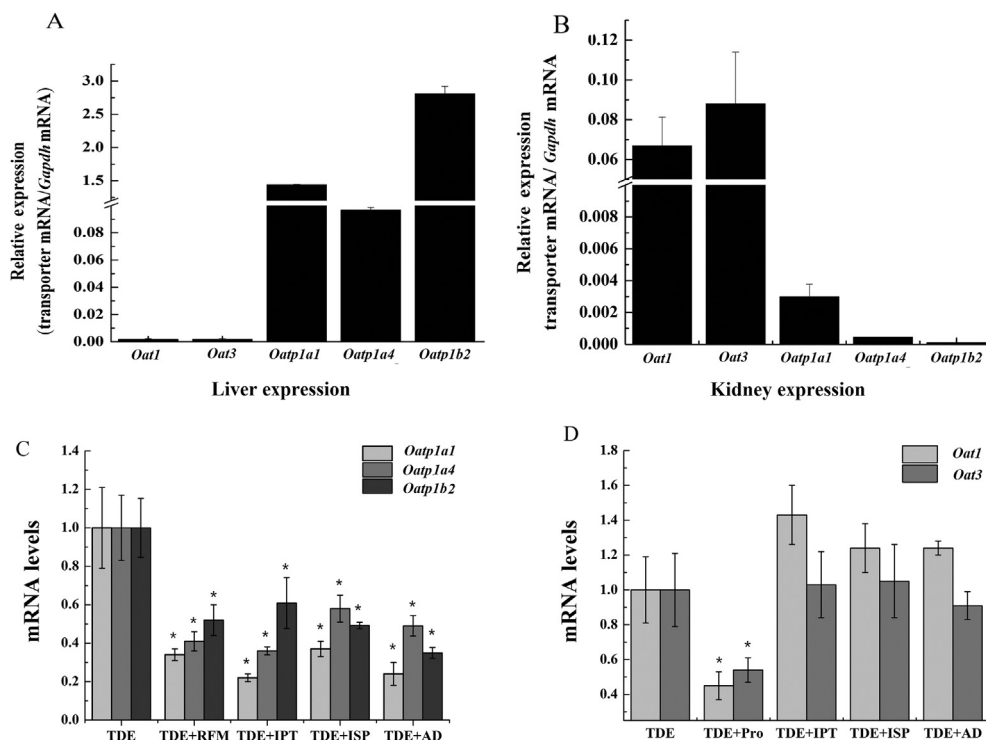
Figure 7 The mRNA levels of mOat1, mOat3, mOatp1a1, mOatp1a4, and mOatp1b2 in liver (A) and kidney (B) of mice. The mRNA levels of mOat1, mOat3, mOatp1a1, mOatp1a4, and mOatp1b2 in mice administrated with TDE in the presence or absence of IPT, ISP, or AD extract in liver (C) and kidney (D) of mice after administrated for 4 h. The values are mean ± SD ($n = 3$); $^*P < 0.05$. Statistical analysis was performed using one-way ANOVA with Bonferroni's *post-hoc* test.

regulation of tight junction proteins. It has been reported that *Ligusticum chuanxiong* Hort (LCH) increased the transport of paeoniflorin by opening tight junctions[22]. Some researchers[23] also found that LCH enhanced the penetrability of echinacoside through the blood−brain barrier model by down-regulating the expression of key proteins responsible for tight junctions of cell membranes, such as claudin five and zonula occludens 1. Those studies explained the mechanism of LCH as messenger drug on how to enhance the efficiency of echinacoside. (3) Drug metabolic enzymes or transporters are the key factors to affect the *in vivo* process of drugs[24]. As the complexity of chemical components in TCMs, many ingredients showed inhibition or induction to the drug metabolic enzymes or transporters, which offered a useful clue for Chinese herb drugs to combine rationally.

Yuanhuzhitong prescription comprised of Rhizoma Corydalis and *A. dahurica* could relieve various pains through activating

or blocking the G-coupled protein receptors (GCPRs) such as 5-HT1A, OPRM1, ADRB2 receptors and block D_2 receptor which are mainly located in the central nervous system[25]. TDE, with bitter property, accounts for the main analgesic activity of Yuanhuzhitong prescription by blocking dopamine receptors in the central nervous system and depleting dopamine within the brain[26,27]. It was suggested that the TDE suppressed pain mainly within the brain region, so it is necessary for TDE to keep a certain concentration in the brain[24,25]. *A. dahurica* with pungent flavor is an important traditional Chinese medicine and can activate blood circulation and take invigorating in the YZP. And what's more, AD has the functions of treating chronic ulcer of soft tissues and antibacterial as well as anti-cancer activity, and it could enhance the central analgesic action of Rhizoma Corydalis[28,29]. Although it was proved that the exposure of TDE could be enhanced significantly when combined with AD extract, the

mechanism was not clear. Here, the authors tried to illustrate the mechanism of the compatibility for ingredients with different properties in the Yanhuzhitong prescription based on the drug−drug interaction mediated by transporters.

In this paper, the authors proved that the main analgesic bioactive substance TDE was the substrate of hOAT3, hOATP1B1, and hOATP1B3 (Fig. 2), while the IPT, ISP, and AD extract showed strong inhibition to the activity of hOAT3 (Figs. 3 and 4). The inhibition of IPT, ISP, and AD extract to OAT3 could decrease the entry of TDE into the kidney when TDE was orally taken in within the Yanhuzhitong prescription, which was certified in the tissue distribution studies (Fig. 6). The inhibition of IPT, ISP, and AD to hOAT3 was competitive, as they did not show a significant effect to the mRNA levels of *Oat1* and *Oat3* of the kidney in mice (Fig. 7). It was suggested that IPT, ISP, and AD extract mainly decreased the accumulation of TDE in kidney by competitively inhibiting the activity of OAT3. The decrease accumulation of TDE in kidney may attribute the enhancement of TDE in plasma and brain. In addition, AD extract also showed strong inhibition to the transport activity of OATP1B1 and OATP1B3 of humans (Fig. 3), which suggested that the transport of TDE from blood to liver was blocked, leading to decreased TDE accumulation in the liver when combined orally with AD (Fig. 6). Although the expression of human OATP1B1, OATP1B3, and OATP2B1 were not detected in the liver of mice, the tissue specificity and substrate recognition of m*Oatp1a1*, m*Oatp1a4*, and m*Oatp1b2* genes are very similar to human *OATP1B1*, *OATP1B3*, and *OATP2B1*. Here, it was showed that the expression of m*Oatp1a1*, m*Oatp1a4*, and m*Oatp1b2* located in the liver were downregulated significantly in the mice treated with TDE in the presence of IPT, ISP, and AD extract (Fig. 7), which may further aggravate the decrease of TDE accumulation in liver to impel more TDE retaining in blood and enter into brain for a better efficacy. These results illustrate the molecular mechanism for the compatibility of different Chinese medicine with different properties such as sour, bitter, pungent and sweet, which may offer a useful reference to reveal the secrets of the compatibility theory.

Acknowledgments

Author contributions

Ze Wang, and Weidang Wu wrote the manuscript. Haihua Shang, and Yan Dong draw the illustrations. Tao Cui, Chen Zhang, and Xiulin Yi contributed to the literature search. Hongbing Zhang, Tiejun Zhang, Xing Huang, Yaping Zhang, and Fengying Yan supplied drugs and reagents. Yazhuo Li and Changxiao Liu edited the manuscript.

Conflicts of interest

The authors report no conflicts of interest.

Appendix A.   Supporting information

Supporting data to this article can be found online at https://doi.org/10.1016/j.apsb.2020.05.012.

References

1. Kim YJ, Lim HS, Kim Y, Lee J, Kim BY, Jeong SJ. Neuroprotective effect of *Corydalis ternata* extract and its phytochemical quantitative analysis. *Chem Pharm Bull* 2017;**65**:826−32.
2. Liu CX, Cheng YY, Guo DA, Zhang TJ, Li YZ, Hou WB, et al. A New concept on quality marker for quality assessment and process control of Chinese medicines. *Chinese Herbal Medicines* 2017;**9**:3−13.
3. Li K, Li J, Su J, Xiao X, Peng X, Liu F, et al. Identification of quality markers of Yuanhu Zhitong tablets based on integrative pharmacology and data mining. *Phytomedicine* 2018;**44**:212−9.
4. Xu H, Li K, Chen Y, Zhang Y, Tang S, Wang S, et al. Study on the absorbed fingerprint-efficacy of Yuanhu Zhitong tablet based on chemical analysis, vasorelaxation evaluation and data mining. *PLoS One* 2013;**8**. e81135.
5. Zhang TJ, Xu J, Shen XP, Han YQ, Hu JF, Zhang HB, et al. Relation of "property−response−component" and action mechanism of Yuanhu Zhitong Dropping Pills based on quality marker (Q-Marker). *Chin Tradit Herb Drugs* 2016;**47**:2199−211.
6. Zhang H, Wu X, Xu J, Gong S, Han Y, Zhang T, et al. The comparative pharmacokinetic study of Yuanhu Zhitong prescription based on five quality-markers. *Phytomedicine* 2018;**44**:148−54.
7. Jia Y, Wang J. Renal drug transporters and their significance in drug−drug interactions. *Acta Pharm Sin B* 2016;**6**:363−73.
8. Hsueh CH, Yoshida K, Zhao P, Meyer TW, Zhang L, Huang SM, et al. Identification and quantitative assessment of uremic solutes as inhibitors of renal organic anion transporters, OAT1 and OAT3. *Mol Pharm* 2016;**13**:3130−40.
9. Wu W, Bush KT, Nigam SK. Key role for the organic anion transporters, OAT1 and OAT3, in the *in vivo* handling of uremic toxins and solutes. *Sci Rep* 2017;**7**:4939.
10. Liu CX, Yi XL, Fan HR, Wu WD, Zhang X, Xiao XF, et al. Effects of drug transporters on pharmacological responses and safety. *Curr Drug Metabol* 2015;**16**:732−52.
11. Sun X, Li J, Guo C, Xing H, Xu J, Wen Y, et al. Pharmacokinetic effects of curcumin on docetaxel mediated by OATP1B1, OATP1B3 and CYP450s. *Drug Metabol Pharmacokinet* 2016;**31**:269−75.
12. Wu WD, Dong Y, Gao J, Gong M, Zhang X, Kong W, et al. Aspartate-modified doxorubicin on its N-terminal increases drug accumulation in LAT1-overexpressing tumors. *Canc Sci* 2015;**106**:747−56.
13. Wu WD, Zhang XY, Wei ZH, Ci XY, Jiang LX, Lu JJ, et al. Inhibition of berberine on organ anion transporters and its bidirectional transmembrane transport. *Drug Evaluation Res* 2017;**40**:778−82.
14. Tan Z, Zhu R, Shi R, Zhong J, Ma Y, Wang C, et al. Involvement of rat organic cation transporter 2 in the renal uptake of jatrorrhizine. *J Pharmacol Sci* 2013;**102**:1333−42.
15. Wu WD, Ci XY, Wei ZH, Zhang XY, Li W, Wang Z, et al. Inhibition effects of anhydroicaritin on important clinical drug transporters. *Drug Evaluation Res* 2018;**41**:986−91.
16. Li LP, Song FF, Weng YY, Yang X, Wang K, Lei HM, et al. Role of OCT2 and MATE1 in renal disposition and toxicity of nitidine chloride. *Br J Pharmacol* 2016;**173**:2543−54.
17. Wang H, Sun P, Wang C, Meng Q, Liu Z, Huo X, et al. Liver uptake of cefditoren is mediated by OATP1B1 and OATP2B1 in humans and Oatp1a1, Oatp1a4, and Oatp1b2 in rats. *RSC Adv* 2017;**7**:30038−48.
18. Chu X, Bleasby K, Evers R. Species differences in drug transporters and implications for translating preclinical findings to humans. *Expet Opin Drug Metabol Toxicol* 2013;**9**:237−52.

19. Chang YX, Sun YG, Li J, Zhang QH, Guo XR, Zhang BL, et al. The experimental study of Astragalus membranaceus on meridian tropsim: the distribution study of astragaloside IV in rat tissues. *J Chromatogr B Analyt Technol Biomed Life Sci* 2012;**911**:71−5.

20. Yang W, Zhang Y, Wu W, Huang L, Guo D, Liu C. Approaches to establish Q-markers for the quality standards of traditional Chinese medicines. *Acta Pharm Sin B* 2017;**7**:439−46.

21. Wu JJ, Guo ZZ, Zhu YF, Huang ZJ, Gong X, Li Y-H, et al. A systematic review of pharmacokinetic studies on herbal drug Fuzi: implications for Fuzi as personalized medicine. *Phytomedicine* 2018;**44**:187−203.

22. Hu PY, Liu D, Zheng Q, Wu Q, Tang Y, Yang M. Elucidation of transport mechanism of paeoniflorin and the influence of ligustilide, senkyunolide I and senkyunolide a on paeoniflorin transport through MDCK-MDR1 cells as blood−brain barrier *in vitro* model. *Molecules* 2016;**21**:300.

23. Zheng Q, Tang Y, Hu PY, Liu D, Zhang D, Yue P, et al. The influence and mechanism of ligustilide, senkyunolide I, and senkyunolide A on echinacoside transport through MDCK-MDR1 cells as blood−brain barrier *in vitro* model. *Phytother Res* 2018;**32**:426−35.

24. Zhang JH, Yu Z, You GF. Insulin-like growth factor 1 modulates the phosphorylation, expression, and activity of organic anion transporter 3 through protein kinase A signaling pathway. *Acta Pharm Sin B* 2020; **10**:186−94.

25. Han YQ, Xu J, Gong SX, Zhang TJ, Liu CX. Chemical constituents and mechanism of Corydalis Rhizoma based on HPLC−QTOF/MS and G protein-coupled receptor analysis. *Acta Pharm Sin* 2016;**51**: 1302−8.

26. Hong Z, Fan G, Le J, Chai Y, Yin X, Wu Y. Brain pharmacokinetics and tissue distribution of tetrahydropalmatine enantiomers in rats after oral administration of the racemate. *Biopharm Drug Dispos* 2006;**27**: 111−7.

27. Zhang Y, Sha R, Wang K, Li H, Yan B, Zhou N. Protective effects of tetrahydropalmatine against ketamine-induced learning and memory injury *via* antioxidative, anti-inflammatory and anti-apoptotic mechanisms in mice. *Mol Med Rep* 2018;**17**:6873−80.

28. Bai Y, Li D, Zhou T, Qin N, Li Z, Yu Z, et al. Coumarins from the roots of *Angelica dahurica* with antioxidant and antiproliferative activities. *J Function Food* 2016;**20**:453−62.

29. Zheng YM, Shen JZ, Wang Y, Lu AX, Ho WS. Anti-oxidant and anti-cancer activities of *Angelica dahurica* extract *via* induction of apoptosis in colon cancer cells. *Phytomedicine* 2016;**23**:1267−74.